EXTRACTION OF SURFACE TOPOGRAPHY FROM SAR STEREO PAIRS USING AN AIRBORNE X-BAND SENSOR: PRELIMINARY RESULTS

A. Schubert[1], D. Small[1], F. Holecz[2], E. Meier[1], D. Nüesch[1]

[1] Remote Sensing Laboratories, University of Zürich; Winterthurerstrasse 190; CH-8057 Zürich; Switzerland
Tel: +41 1 635 6523 FAX: +41 1 635 6842, Email: {schubert,daves,meier,nuesch}@geo.unizh.ch
[2] sarmap s.a.; Cascine di Barico; CH - 6989 Purasca; Switzerland
Tel: +41 91 600 9366 FAX: +41 91 600 9369, Email: francesco.holecz@sarmap.ch

ABSTRACT

The two most reliable methods for extracting surface topography from SAR image pairs are interferometry and stereogrammetry. Although the high-resolution results obtained by interferometry have been the main focus for research into digital surface model (DSM) generation in recent years, it has been shown that the use of a lower-resolution DSM, obtained in this study by processing a SAR stereo pair, can aid in the generation of an interferometric DSM. In addition, height information for areas where the interferometric technique fails is often available in a stereogrammetrically-derived DSM. Because of the increasing availability of stereoscopic and interferometric coverage generated by air- and spaceborne sensors in the near future, the combination of radargrammetric stereo SAR with interferometry is becoming more feasible.

This paper describes the extraction of high-resolution topographical information from SAR imagery, using stereogrammetry based on multiresolution wavelet-matching. The data were obtained by a single airborne sensor over a test site in Switzerland. The resulting stereogrammetric DSMs are compared to an existing interferometric DSM. The limits of the stereoscopic technique are further investigated through simulation of the radar backscatter using a reference digital elevation model (DEM) and nominal backscatter values mapped from the DEM into radar geometry. Sources of possible geometric errors in the stereo DSMs are studied.

It is concluded that using a multiresolution stereo matching approach combined with good sensor positioning information makes automatic generation of a high-quality DSM possible. The latter can subsequently be used to improve the accuracy of a high-resolution InSAR-derived height map.

INTRODUCTION

Extracting surface height information from SAR-amplitude stereo pairs dates back to work done in the 1960s, pioneered by La Prade [1], and is described in detail by Leberl [2]. Computing technology has only more recently made it possible to automate the process digitally. Satellites such as ENVISAT-1 and RADARSAT-1 are quickly increasing the availability of near-simultaneous stereo SAR and InSAR data. This has caused a recent surge of interest in height-extraction techniques based on the fusion of stereo and InSAR (for examples, see [3] and [4]).

The motivation for pursuing the integration of stereo within an InSAR framework is to overcome the weaknesses inherent in the latter method, namely:

- Ground control points (GCPs) are required for interferometric **phase calibration**; the stereo matching algorithm used here is fully automatic.
- InSAR topography estimation requires a delicate **phase-unwrapping** step, which can be greatly aided by an existing low-frequency DSM such as may be provided by stereogrammetry.
- Areas of **low coherence** in interferograms, especially due to temporal decorrelation during multi-pass InSAR or vegetation presence, are topographically unresolvable or provide unsatisfactory height estimates at best. This is not a problem inherent to stereo SAR.

Stereogrammetry relies on image matching, which does not always provide accurate parallax estimation in areas with few features. However, with a coarse-to-fine matching implementation using wavelets, which are by their nature sensitive to phenomena at multiple scales, even homogeneous image regions can be properly matched as long as they are bounded by recognisable features or textures, and do not dominate the image. The SNR of the disparity field over these regions can be improved by an adaptive smoothing process during coarse-to-fine matching, at the cost of poorer resolution in the final product.

Therefore, although a stereo DSM will not provide nearly the height resolution of an InSAR DSM, InSAR processing can benefit from the availability of stereo.

The scope of this paper does not extend beyond stereo processing. The Remote Sensing Laboratories at the University of Zurich has many years of experience in InSAR processing and topography estimation, and the necessary software and know-how is available. However, the implementation of a stereo processing chain is a recent addition, and its fine-tuning is still under way. Its

subsequent merging with the existing InSAR processor is expected to be a relatively smooth process.

STEREO SAR PROCESSING

The processing chain consists of the following steps:

- SAR focusing with motion compensation
- Choice of image pair suitable for stereogrammetry
- Speckle reduction
- Coarse mapping of slave into master geometry
- Coarse radiometric adjustment of slave with respect to the master radiometry
- Disparity field (parallax) estimation
- Height map generation and geocoding

Fundamental requirements for achieving the theoretical resolution of the system are the availability of high precision DGPS and high frequency attitude data of the platform, the precise measurement of the antenna positions with respect to the GPS system, knowledge of exact time synchronization and range delay, and the consideration of all related geodetic and cartographic transforms.

Based on the post-processed real platform positions collected by the navigation system, an ideal flight path is generated. Motion displacements in range and azimuth direction as well as velocity variations with respect to these ideal flight paths are then calculated. Successively, the motion instabilities of the platform are corrected, before the SAR focusing step.

The stereogrammetric processing consists of the disparity estimation, or matching, and its subsequent conversion to heights in a map geometry through one of two paths: simplified analytic calculation of a slant-range height map and its conversion to map geometry, or direct estimation of map heights by numerically solving the range-Doppler equations for the stereo geometry.

DISPARITY FIELD ESTIMATION

The image matching problem has been studied actively for the last 20 years by researchers in fields such as computer vision, medicine, biology, and remote sensing because of the need to correlate images that vary slightly from one to the next, either spatially or temporally. The matching algorithms described in the literature can be roughly classified as being area- or gray-level-based, feature-based [5], or hybrids. Their implementation within multiresolution, or coarse-to-fine frameworks has led to hybrid algorithms that now make stereo matching all the more feasible.

The matching approach used during this work was first outlined by H-P. Pan in 1996 [6], which he called *uniform full-information image matching.* It depends on a wavelet multiresolution decomposition of the image. A complex discrete wavelet transform using Magarey-Kingsburys wavelets [7] is calculated for the pair, which produces lossless representations of the images on multiple resolution levels. At each level a new quarter-resolution approximation image is generated, as well as three detail images of the same size, permitting lossless reconstruction of the image from the previous level. By minimising the *similarity distance* for all homologous points at all levels of resolution beginning with the coarsest level, we incrementally fine-tune the estimated disparities at each finer level, eventually generating a disparity field for the image pair at one quarter the original resolution. At each level of matching, the disparity field is regularised to provide a global compromise between feature similarity and disparity field continuity. This regularisation, described for example in [8], was an improvement on the original algorithm and reduced the signal-to-noise ratio of the subsequent height reconstructions. This improved version of the algorithm was found to be quite well adapted to radar amplitude image pairs, as long as the slave image was first transformed into the slant-range reference frame of the master image before matching. This transformation is necessary in order to remove the first-order geometric differences between the two images arising from their different look angles. The resulting disparity field describes the range differences between the two sensor positions and the pixel ground locations.

HEIGHT MAP GENERATION

For a given homologous pixel pair, the horizontal, or range, component of the disparity field generated by the matching process is a direct measurement of the difference in range from that point to each of the sensors. Given these range differences for all points, and given accurate flight position and velocity information, the following four equations must be satisfied for each pair of homologous points:

$$\left|\vec{P} - \vec{S}_1\right| - \left|\vec{r}_1\right| = 0 \tag{1}$$

$$\frac{-2}{\lambda} \cdot \frac{(\vec{P} - \vec{S}_1)(\vec{v}_{S_1})}{\left|\vec{P} - \vec{S}_1\right|} + f_{d_1} = 0 \tag{2}$$

$$\left|\vec{P} - \vec{S}_2\right| - \left|\vec{r}_1\right| - \delta_r = 0 \tag{3}$$

$$\frac{-2}{\lambda} \cdot \frac{(\vec{P} - \vec{S}_2)(\vec{v}_{S_2})}{\left|\vec{P} - \vec{S}_2\right|} + f_{d_2} = 0 \tag{4}$$

where:

$\vec{P}$	=	ground point positions
1, 2	=	master (1) and slave (2) antenna
$\vec{S}$	=	antenna positions
$\vec{r}$	=	slant ranges $\vec{P}$ to $\vec{S}$
$\vec{v}$	=	sensor velocities relative to $\vec{P}$
f_d	=	Doppler frequencies
δ_r	=	range differences (disparities)
λ	=	radar wavelength

These equations are over-determined, but may be solved numerically, taking into account the non-zero squint for each sensor. The solution of the four equations for the case of a non-zero squint geometry yields a height for each homologous pair in an Earth-centred global cartesian reference system [9]. This geo-referenced height field is then transformed into a Swiss map geometry to allow comparison with other available height models.

SAR SYSTEM AND DATA

This airborne InSAR system was designed and manufactured at Aero-Sensing Radarsysteme GmbH. The characteristics of the AeS-1 SAR system during acquisition of the data used in this study are shown in Table 1.

Frequency [GHz]	9.6
Polarisation	HH
Bandwidth [MHz]	400
Swath width [km]	2.2
Incidence angle [deg]	45
PRF [Hz]	10320
Radiometric resolution [dB]	1.8-1.0
Positioning	DGPS and IMU

Table 1: SAR system parameters

In particular the following features of this InSAR system have to be considered:

- The maximum selectable system bandwidth allows a ground range resolution of better than 0.5 meters.
- The platform is equipped with integrated real time Differential Global Positioning System (DGPS) and an Inertial Motion Unit (IMU). This provides extremely accurate positioning information of the platform.

The AeS-1 InSAR data of the site 'Küttigkofen', in northwestern Switzerland (47.2^{o}N, 7.5^{o}E), were acquired on April 24th, 1999 using a range bandwidth of 400 MHz and 2.2 km swath width. The site is located between the cities of Solothurn and Berne and covers an area of about 6 km^2. The area was chosen according to the following criteria:

- Terrain ranging from flat to hilly with height differences of up to 150 meters and several different terrain features and ground cover types.
- Digital land registry data of 1:5000 scale (grid size 1m) available.
- Digital surface model (DSM) data, collected on July 1st 1999, having a grid size of 1m and height resolution of 0.1m available.

RESULTS AND DISCUSSION

The height model used to validate the results was obtained using the DoSAR airborne InSAR system from Dornier (for a description of this system and DSM generation using it, refer to [10]). Figure 1 shows the DoSAR height model for the Küttigkofen test site.

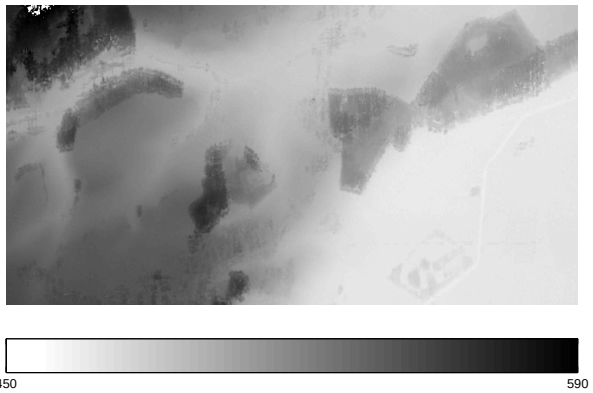

Fig. 1. The DoSAR digital surface model [m]

The high quality of the DoSAR model was established by comparing it at various locations to ground control points (GCPs) with precisely-known positions. Table 1 summarises the statistics for 169 GCPs distributed across the entire DoSAR scene.

Number of points used	169
Total area covered [km^2]	210
Mean height difference [m]	-0.040
Mean absolute height difference [m]	0.795
Standard deviation [m]	1.044

Table 2: Validation of the DoSAR DSM using GCPs distributed over the entire scene

It was found that the multiresolution matching approach, implemented in MATLAB, was well-adapted to the SAR image pair used during this study. Even without speckle reduction (using a 5x5 Frost filter), the matches found by the algorithm resulted in accuracies of one pixel or better over most of the image. This was verified by using the estimated disparity field to resample the slave image and comparing the result to the master image. It was possible to compare the pixel positions of bright corner reflectors in both scenes manually, and in all cases an ac-

curacy of one pixel or less was noted. Figure 2 shows the master, resampled slave, and the difference between them for a part of the Küttigkofen scene. The almost perfect absence of bright pixels in the difference indicates a good correspondence was found between the master and slave images. It is important to note that because of radiometric differences between the two input images arising

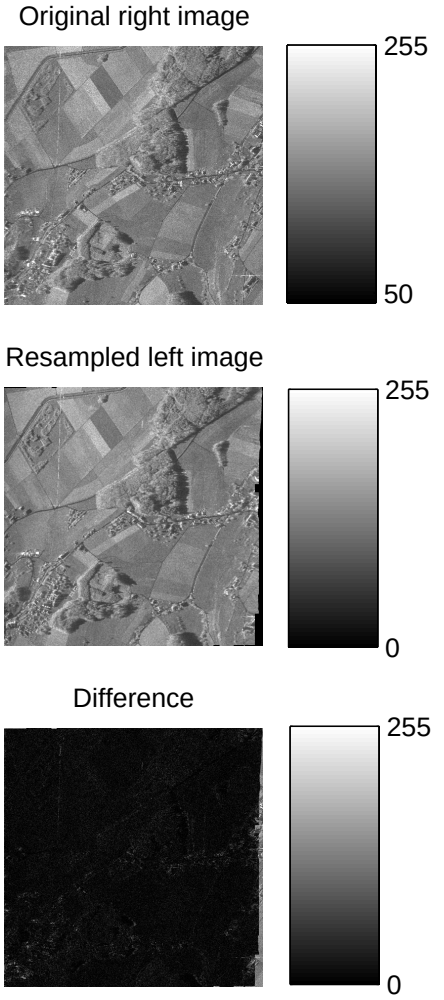

Fig. 2. Master image, resampled slave, and their difference (8-bit grayscale levels)

from the different view geometries and speckle, even a perfect match - which is defined purely geometrically as a vector field - does not result in a resampled slave that exactly matches the master *radiometrically*. In this sense it is more convincing to manually compare image positions of individual homologous pixel pairs.

In order to evaluate the performance of the height reconstruction process given a disparity field under controlled conditions, a radiometric SAR image simulator, described in [11], was used to create a stereo pair with geometric properties identical to those of the real pair. The DoSAR DSM was used to generate the simulations. As can be seen in Figure 3, the most obvious difference between a real and simulated image is the lack of information in areas where the backscatter depends on the surface characteristics. This is to be expected, since the DoSAR DSM contains no information about the landcover. In spite of this, the matching algorithm was observed to work nearly perfectly even in image areas with few features or textural variations.

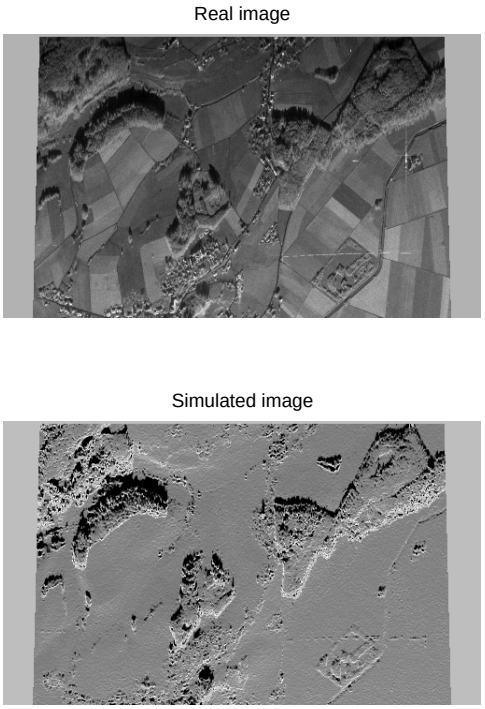

Fig. 3. Real image and simulation of the same scene

The resulting disparity field for the simulated pair was then used to geocode the scene into Swiss map geometry, by solving Equations (1) through (4) as described earlier. Figure 4 shows the resulting height map. The differences between it and the DoSAR reference are shown in Figure 5; the error statistics are summarised in Table 3.

The equivalent results for the DSM obtained using the real image pair are shown in Figure 6, Figure 7, and Table 4.

The most striking features of both Figures 5 and 7 is that the heights of the three forest stands visible in the images are consistently underestimated, and the radar shadow regions are overestimated.

The radar shadows above the northern edges of these regions are assigned heights much greater than the ground level over which they lie. This is to be expected, since the shadows ‘appear’ to stem directly from the northern edges of the forest stands, resulting in a parallax between the shadow regions equal to the parallax between the stand northern tree edges themselves. In this sense, the heights erroneously assigned to the shadows

will approximate the stand heights along their northern edges.

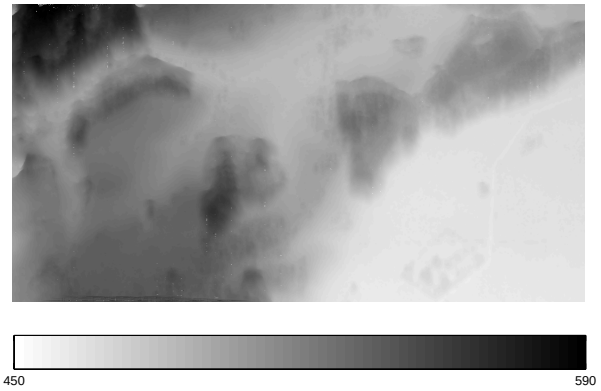

Fig. 4. DSM obtained using the *simulated* pair [m]

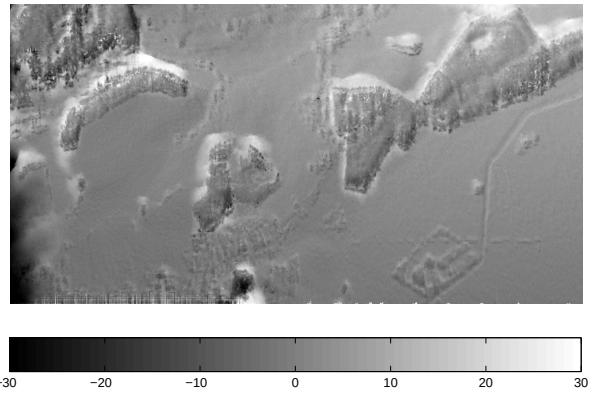

Fig. 5. Height error for the *simulated* pair (m)

Mean height error [m]	-2.7
Standard deviation [m]	18.3
Points with < 5m error [%]	56.1
Points with <20m error [%]	86.1
Points with <50m error [%]	94.0

Table 3: Error statistics for DSM obtained from the simulated pair

More surprising is the consistent height underestimation of the forest stands and relatively large amount of noise, even in the simulation reconstruction. It can only be concluded that a geometric error is present in the current geocoding process. This is supported by the following facts:

- The matching has been shown to be accurate to one pixel or less.
- The same flight path and motion information used to simulate the stereo pair was used during geocoding.
- The motion and Doppler centroid data corresponding to the motion-compensated amplitude pair have been verified as being correct to within one pixel.

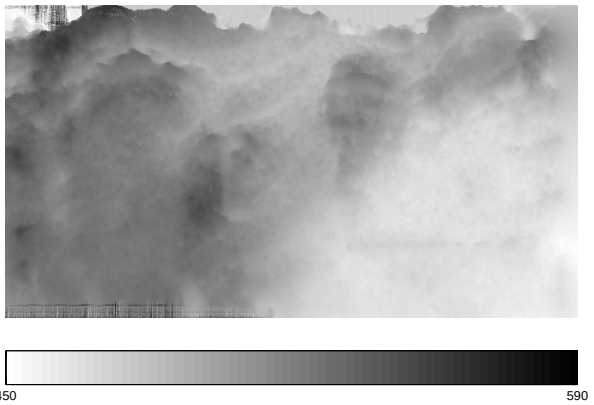

Fig. 6. DSM obtained using the *real* pair [m]

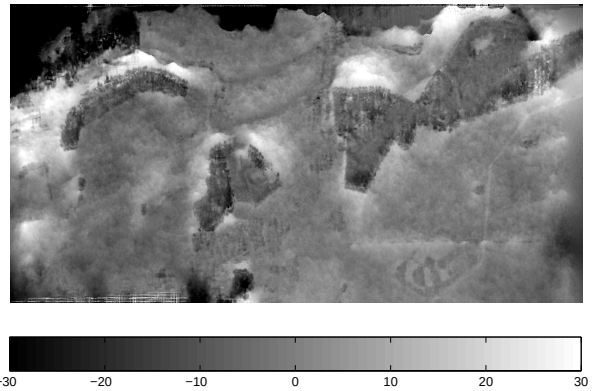

Fig. 7. Height error for the *real* pair [m]

Mean height error [m]	-6.9
Standard deviation	23.1
Points with < 5m error [%]	45.6
Points with <20m error [%]	86.4
Points with <50m error [%]	95.2

Table 4: Error statistics for the DSM obtained from the real pair

Based on this information, and in light of the results, it is clear that the DSMs obtained are not yet of the quality that should be obtainable with the available data.

This conclusion is reinforced by Figure 8. The general trend of height underestimation in proportion to true height is clearly visible, and is indicated by a linear least-squares fit. The vertical arm-like structures springing

from the central region are due to random noise about fixed height levels such as the ground, shadow effects, and random height estimation errors near the image edges.

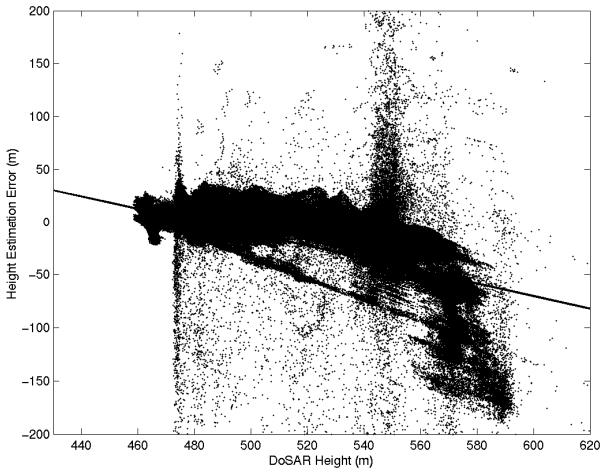

Fig. 8. Height error versus DoSAR height for the DSM obtained from the real pair, with least-squares-fit line

CONCLUSIONS AND OUTLOOK

The central requirements for obtaining a DSM of a resolution near the theoretical limits of the system using stereogrammetry have been met. Given a pair of SAR amplitude images suitable for stereogrammetry, these are:

- the ability to find the correspondence between the two images that brings one into alignment with the other (stereo matching)
- the availability of accurate positioning information for the sensor over both scenes

These conditions are the most difficult to satisfy in the context of stereo SAR processing in general. Therefore, it can be stated that the stereo processing problem has effectively been solved. The matching and geocoding are possible without GCPs, and provide height estimates for all image locations. It is expected that the geometric error observed in the results so far will quickly be rectified, and subsequent work will focus on the integration of the stereo processing chain into the already-existing InSAR framework.

The radiometric simulations will be made more realistic by implementing a landcover-dependent backscatter mechanism. This will fill in the homogeneous regions visible in the current simulated images with radiometric variations closely linked to the type of landcover (soil, crops, etc.), based on backscatter statistics for the landcover types encountered.

By adjusting the stereo baseline in the simulations, it will be possible to determine to what extent the acquisition geometry plays a role in the quality of the resulting stereogrammetric height map.

REFERENCES

[1] La Prade G., 1963. An analytical and experimental study of stereo for radar. Photogrammetric Engineering and Remote Sensing 29(2), pp. 294-300.

[2] Leberl F.W., 1990. Radargrammetric image processing. Artech House, Los Angeles, USA, Chapters 12-13.

[3] Gelautz M., Paillou Ph., and Chen C., 1999. Topographic Surface reconstruction using interferometric and stereo techniques. Proc. IGARSS'99.

[4] Elizavetin I.V., 1999. Merging of stereo and interferometric processing for improved DEM generation. Proc. IGARSS'99, pp. 2099-2107.

[5] Toutin T., Gray L., 2000. State-of-the-art of elevation extraction from satellite SAR data. ISPRS Journal of Photogrammetry and Remote Sensing 55(2000), pp. 13-33.

[6] Pan H-P., 1996. General stereo image matching using symmetric complex wavelets. Wavelet applications in signal and image processing IV, Proc. SPIE 2825, 1996.

[7] Magarey J., Kingsbury N., 1996. Motion estimation using a complex-valued wavelet transform. Wavelet applications in signal and image processing IV, Proc. SPIE 2825, 1996.

[8] Magarey J., Dick A., 1998. Multiresolution stereo image matching using complex wavelets. International Conference on Pattern Recognition no. 14, 1998.

[9] Holecz F., Pasquali P., Moreira J., Meier E., Nüesch D., 1998. Automatic generation and quality assessment of digital surface models generated from AeS-1 InSAR data. Proc. EUSAR'98, pp. 57-60.

[10] Goblirsch W. et al, 1995. Accuracy of interferometric elevation models generated from DoSAR airborne data. Proc. IGARSS'95, pp. 770-774.

[11] Small D., 1998. Absolute radiometric correction in rugged terrain: a plea for *integrated* radar brightness. Proc. IGARSS'98, pp. 330-332.